Advance Sustainable Science, Engineering and Technology (ASSET)
Vol. 8, No.2, April 2026, pp. 02602023-01 ~ 02602023-019
ISSN: 2715-4211 DOI: https://doi.org/10.26877/asset.v8i2.2638

Numerical Simulation of Mixed Convection Heat Transfer in a Vehicle Cabin with Variable Aspect Ratios Using CFD

Sarmad Ahmed Ali [1*], Riyam Basim Al-Tameemi [2], Maithem Hussien Rasheed [3], Ali M. Ashour [4]

[1]Automobile Engineering Department, College of Engineering-Al Musayab, University of Babylon, Province of Babylon, 51001 Hillah, Iraq.

[2]Imam Alkadhim University College, Province of Baghdad, 14522, Iraq.

[3]Department of Energy and Renewable Energies, College of Engineering-Al Musayab, University of Babylon, Province of Babylon,51001, Iraq.

[4]Department of Mechanical Engineering, Faculty of Engineering, University of Technology, Province of Baghdad, Iraq.

*sarmad.ahmed96@uobabylon.edu.iq

Abstract. The study of mixed convection heat transfer within rectangular cavities is a vital topic in engineering applications such as ventilation systems and heat exchangers. In this research, ANSYS Fluent software was used to simulate heat transfer within a rectangular cavity. The left wall was heated, and the right wall was cooled; the aspect ratio (AR) was varied (0.5-2), and an inlet was installed at the top and an outlet at the bottom, while the other walls were insulated. The Reynolds number (Re) values ranged from (4000 to 22000), and the Richardson number (Ri) ranged from (10 to 1200). The results showed that the Nusselt number increased with increasing Re and decreased with Ri, reaching a maximum of 185.3 at AR = 0.5 and Re = 21312, while the highest thermal efficiency of 0.284 was recorded at AR = 1 and Re = 4736. The flow and temperature contour also revealed that AR = 1 provides an optimal balance between heat transfer enhancement and flow stability, making this ratio most suitable for the design of a highly efficient thermal system.

Keywords: vehicle cabin, thermal management, turbulent flow regime, reynolds number, aspect ratio, CFD simulation

(Received 2025-08-28, Revised 2026-01-14, Accepted 2026-01-20, Available Online by 2026-04-27)

1. Introduction

Mixed-convection heat transfer is a complex thermal phenomenon that arises from the interaction between forced convection, caused by fluid motion due to external sources, and free convection, caused by density differences resulting from a thermal gradient. The car cabin is a relatively closed environment, and its heat distribution is significantly influenced by the design of the ventilation system, the location of the air vents, and the temperature difference between the interior surfaces. Understanding this phenomenon is of great practical importance in improving passenger comfort and reducing energy consumption in heating and cooling systems [1], [2], [3], [4], [5].

Previous studies on mixed convection in channels and cavities with the effect of wall motion and source location on heat transfer will be reviewed. JF Hinojosa et al. [6] conducted an experimental and numerical study that examined the heat transfer and airflow characteristics of turbulent mixed convection within a ventilated cavity. Air was used as the heat transfer fluid, with a uniform heat flow applied to a vertical wall opposite a constant-temperature wall, while the other walls remained thermally insulated. The results showed that the standard k–ε turbulence model provided the best agreement with the experimental data, with differences not exceeding 3%. The heat transfer coefficient ranged from 2.2–3.4 W/m²K, increasing with increasing Rayleigh and Reynolds numbers. Numerical analyses confirmed that the agreement between the experimental and numerical results was higher at higher inlet velocities, highlighting the effect of varying Rayleigh and Reynolds numbers on the flow patterns and temperature distribution. Lounes Kouf et al. [7]mixed convection heat transfer was numerically studied within ventilated cavities with inlet and outlet openings under four different port configurations. The researchers used the RNG k–ε turbulence model with the finite volume method to study the effects of ventilation and heating at high Rayleigh numbers. The results showed that configuration D provided the best thermal distribution and ventilation efficiency, while configurations A and C were suitable for winter conditions, and configuration B performed well in temperate climates.

Antonio Carozza [8] unsteady mixed convection phenomenon was numerically investigated inside a two-dimensional open cavity with different geometric dimensions, where the temperature on the side walls was held constant while the other surfaces were thermally insulated. The solution was performed using the finite volume method and the SIMPLE algorithm for a wide range of Reynolds numbers (100–1000) and Richardson numbers (0.132–6.5×10^2) with different cavity aspect ratios. The results showed that the heat transfer rate increases significantly with increasing Reynolds number, and the assisted configuration was found to be more thermally efficient than the counter-convection configuration. Bengisen Pekmen Geridonmez and Hakan F. Oztop [9] mixed convective flow in a shroud-driven cavity under the influence of a uniform partial magnetic field was numerically analyzed using a pseudo-spectral method based on vector basis functions. The cavity was designed as a two-dimensional square with insulated horizontal walls and constant-temperature vertical walls, while the upper wall moved in the positive or negative x-direction. The study investigated the effects of Hartmann number and Richardson number, along with the length and location of the partial magnetic field, on the flow behavior and heat transfer. The results showed that increasing the magnetic field length or its centring in the cavity reduced the convective heat transfer. Furthermore, it was found that shroud movement in the negative x-direction had a weaker effect on the convection compared to the positive x-direction.

Nikita S. Gibanov et al. [10] studied mixed convection inside a square cavity containing a triangular porous layer and a local heater. The finite-difference method was used to formulate the flow, vorticity, and temperature functions to solve the governing equations. The influence of Richardson and Darcy numbers, heater length, and porous layer location on the streamlines, temperature distributions, and local and average Nusselt numbers was analyzed. The results showed that these factors significantly influence the flow patterns and heat transfer within the cavity. Hicham Doghmi et al. [11] examined mixed convection heat transfer within a ventilated three-dimensional cavity using the finite volume method, focusing on the influence of certain thermal and geometric parameters. The study covered a low Reynolds number (100), with the Richardson number varying over a wide range from very low (0.01) to high (up to 10). The role of the aperture dimensions was also analyzed, with a constant relative height

of 1/8 of the cavity length and a variable relative width ranging from half the length to the full length. The results showed that heat transfer and flow intensity improvement directly depend on the optimal selection of these parameters, as balancing them leads to higher Nusselt number values and enhanced thermal efficiency of the cavity.

Rongjia Zhu et al. [12] demonstrated the mixed-convection behavior at high Richardson numbers in metallic reactors, using experimental data for a smelter-like vessel at $Re \approx 47$ and $Gr \approx 1.1\times10^{10}$ with dibenzyl toluene fluid. The results showed that the k–ω SST turbulence model achieved the best agreement with the experiments, and that the buoyancy effect was the dominant factor on flow and heat transfer, while the effects of non-buoyancy factors were less pronounced. Ka Lok Lee et al. [13] studied the effects of wind speed (0–9 m/s), deflection angle (0° and 90°), and inclination angle (15° and −90°) on heat losses from a heated cylindrical cavity with different inner wall temperature distributions. The results showed that the heat distribution had a significant effect on losses, with a change of up to 50% in zero or sideways winds, while it decreased to about 20% in high-incline, headward winds. Downward-sloping cavities lost approximately three times more heat than upward-facing cavities.

N. A. Bakar et al. [14] analyzed the effect of a magnetic field on fluid flow and heat transfer within a two-dimensional square cavity, where the vertical walls remained insulated, the upper wall at a low temperature, and the lower wall at a high temperature ($T_h > T_c$). The results showed that the magnetic field affects the streamlines and temperature distribution, as well as the Nusselt number values on the hot and cold walls. Somayeh Davoodabadi Farahani et al. [15] studied mixed convection heat transfer in a rectangular chamber with sinusoidally oscillating walls and mechanical vibrations, using the finite volume method to analyze the effects of frequency, amplitude, Rayleigh number, and fluid type on the Nusselt number. The results showed that sinusoidal hot wall vibrations and transverse chamber earthquakes increased heat transfer by approximately 96% and 75%, respectively, with amplitude having a greater effect than frequency. Nu was estimated with high accuracy using the GMDH model ($R^2 = 0.948$).

References [16], [17], [18], [19], [20] studied mixed convection in horizontal, square, and triangular channels and cavities with localized heat sources and moving or fixed walls, focusing on the effects of Richardson and Reynolds numbers, the location and shape of the heat sources, the presence or absence of wall motion, and wall properties such as emissivity. The results showed that moving walls or changing the location of the sources significantly enhances heat transfer, with a greater effect in some cases, such as a moving left wall or the presence of a heat sink. However, the temperature distribution and heat transfer rates depend on the source location and the properties of the walls and air. Mohammad Nahidul Islam et al. [21] investigated the heat flow behavior in a square cavity with a heated base and a central bulge. The results showed that increasing the Grashof number enhances natural convection and the formation of secondary eddies, while a higher Reynolds number strengthens forced flow, potentially reducing the effect of natural convection. The Prandtl number was also found to significantly influence heat transfer; low values produce smooth heat fields, while high values lead to steep temperature gradients. The bulge at the base enhanced local circulation and improved heat mixing, increasing the average Nusselt number by up to 45% compared to a cavity with a flat base. This highlights the importance of engineering modifications for optimizing heat transfer in applications such as electronics cooling, energy storage, and HVAC system design.

This work will investigate mixed-convection heat transfer within a two-dimensional model representing a simplified car cabin, focusing on turbulent flow over Reynolds number ranges of (4000 to 22000). The effect of the aspect ratio on thermal performance will also be investigated. Simulations will be conducted using the finite volume method (FVM) using ANSYS Fluent to obtain temperature distributions, velocity vectors, local pressure, effectiveness, and average Nusselt numbers. The effects of inlet velocity and geometry on heat transfer behavior will then be analyzed. Although previous studies have addressed the effect of wall movement, source location, and geometric dimensions on mixed convection heat transfer, the gap lies in not studying the effect of changing the aspect ratio of a rectangular cavity with the left wall heated, the right wall cooled, and the presence of an air inlet at the top and an air outlet at the bottom while insulating the remaining walls, which is the subject of the

current research.

2. Methods

2.1 Physical Description of Problem

The model under consideration is a closed rectangular cavity representing a simplification of a car cabin, with variable length and a constant height of 2 m to achieve different aspect ratios (0.5, 1, 1.5, and 2). The working fluid used is air at a reference temperature of (300 K). The right wall of the cavity is cooled at (300 K), while the left wall is heated to a constant temperature of (320 K). The fluid inlet is located at the top of the left wall, while the outlet is located at the bottom of the right wall. The remaining walls (top, bottom, and parts of the walls without openings) are thermally insulated. This characterization aims to study the effect of varying aspect ratios, as well as the inlet fluid velocity, on heat transfer and air movement within the space, taking into account the combination of forced convection resulting from the incoming air flow and free convection resulting from temperature differences between the walls. Figures (1 and 2) show a two-dimensional cavity as the aspect ratio changes. This change aims to study the effect of the cavity's geometric shape on the natural convection heat transfer mechanism, as a change in the aspect ratio leads to a change in the flow distribution and temperature distribution within the cavity.

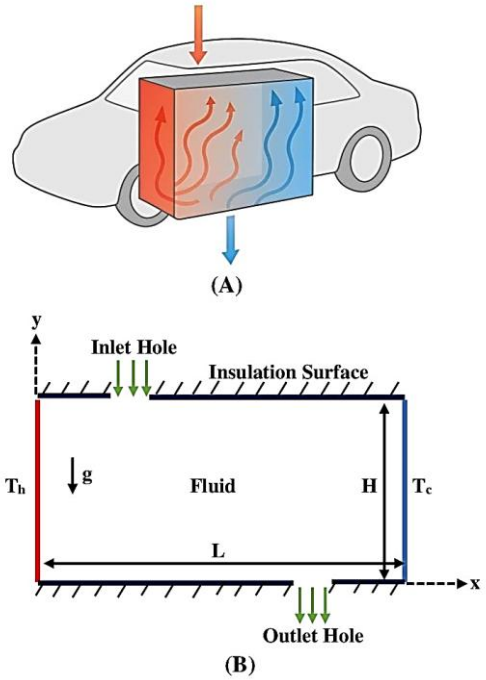

Figure 1. Numerical scheme of mixed heat flow and convection in: (A) vehicle cabin and (B) rectangular cavity with input and output holes.

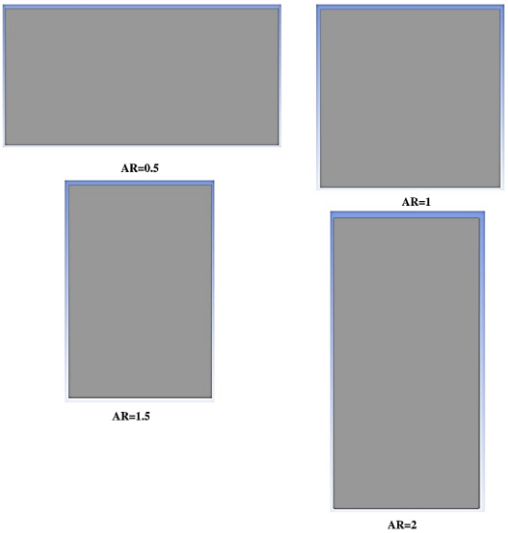

Figure 2. Two-dimensional cavity configurations at different aspect ratios.

2.2 Boundary Conditions and Parameters Studied

Turbulent airflow was assumed within the cavity, with Reynolds numbers ranging from Re = 4000 to Re = 22000, with increments of 200 between each case. The fluid inlet temperature was set at 300 K, while the outlet temperature was not imposed but calculated numerically as a result of the fluid's interaction with hot and cold surfaces within the cavity. The right wall of the cavity was cooled to (Tc = 300 K), while the left wall was heated to a constant temperature of (T_h = 320 K). All other walls (including the ceiling and floor) were thermally insulated. The inlet at the top of the left wall was represented by a constant velocity inlet, with the velocity varying to achieve the desired Reynolds number values, while the outlet at the bottom of the right wall was represented by a constant pressure outlet at the reference atmospheric pressure. The properties of the fluid (air) were kept constant at a reference temperature of 300 K, with the appropriate values of density, viscosity, heat capacity, and thermal conductivity being adopted for that temperature[22], [23], [24] . Table (1) shows the boundary conditions adopted in the current study, which include the geometric properties of the cavity, thermal wall conditions, flow type, in addition to the properties of the fluid used and the boundaries of the flow inlets and outlets.

Table 1. Table of boundary conditions and physical parameters adopted in the study.

Parameter	Symbol	Value/field	Unit	Note
Length of cavity	L	4, 2, 1.333, 1	m	------
Height of cavity	H	2	m	Constant for all cases
Aspect Ratio	AR	0.5, 1, 1.5, and 2	------	AR=L/H
Hot wall temperature	T_h	320	K	Left wall
Cold wall temperature	T_c	300	K	Right wall
Type flow	Turbulent	------	------	------
Reynolds number range	Re	4000-22000	------	------
Inlet hole	------	Velocity inlet	m/s	------
Outlet hole	------	Pressure outlet	Pa	Atmospheric pressure
Insulation walls	------	$\frac{\partial T}{\partial y} = 0$	------	Upper and lower walls

Fluid	------	air	------	Constant properties at 300 K
Densify	ρ	1.177	kg/m^3	at 300K
Dynamics viscosity	μ	1.846 x10^{-5}	Pa.s	at 300K
Heat capacity	Cp	1007	J/kg.K	at 300K
Thermal conductivity	λ	0.0262	W/kg.K	at 300K

2.2.1 Governing and Dimensionless Equations

The problem is solved using the equations of flow and heat transfer for mixed convection, assuming laminar flow, a Newtonian fluid, and steady-state conditions. The governing equations are [25], [26], [27]:

Continuity equation (mass conservation):

$$\frac{\partial u}{\partial x}+\frac{\partial v}{\partial y}=0 \qquad (1)$$

Momentum equation (conservation of momentum) in the x and y directions:

$$\rho\left(u\frac{\partial u}{\partial x}+v\frac{\partial u}{\partial y}\right)=-\frac{\partial p}{\partial x}+\mu\left(u\frac{\partial^2 u}{\partial x^2}+v\frac{\partial^2 u}{\partial y^2}\right) \qquad (2)$$

$$\rho\left(u\frac{\partial v}{\partial x}+v\frac{\partial v}{\partial y}\right)=-\frac{\partial p}{\partial x}+\mu\left(u\frac{\partial^2 v}{\partial x^2}+v\frac{\partial^2 v}{\partial y^2}\right)+\rho g\beta\left(T-T_c\right) \qquad (3)$$

Energy equation (conservation of heat energy):

$$\rho C_p\left(u\frac{\partial T}{\partial x}+v\frac{\partial T}{\partial y}\right)=k\left(\frac{\partial^2 T}{\partial x^2}+\frac{\partial^2 T}{\partial y^2}\right) \qquad (4)$$

The k–ε turbulence model was used in numerical simulations to study mixed-convection heat transfer. This model is one of the most popular and effective turbulence models for dealing with turbulent flows inside cavities and channels. The model is based on solving two energy conservation equations: the turbulence kinetic energy (k) and its decay rate (ε). This allows for estimating the effect of turbulence on fluid velocity and heat transfer within the studied range. This model provides good accuracy in representing the velocity and temperature distributions in turbulent flows within reasonable limits of computational complexity [28], [29], [30], [31].

$$\rho_{nf}\left(\frac{\partial \vec{V}}{\partial t}+\vec{V}.\nabla\vec{V}\right)=-\nabla p+\nabla.[(\mu_{nf}+\mu_t)(\nabla\vec{V}+(\nabla\vec{V}))^T]+\rho_{nf}\,\vec{g}\,\beta(T-T_{ref}) \qquad (5)$$

$$\rho_{nf}C_{p,nf}\left(\frac{\partial T}{\partial t}+V.\vec{\nabla}T\right)=\nabla.\left[\left(k_{nf}+\frac{C_p\mu_t}{\mathrm{Pr}_t}\right)\nabla T\right] \qquad (6)$$

$$\frac{\partial k}{\partial t}+\vec{V}.\nabla k=\nabla.\left[(\nu+\frac{\nu_t}{\sigma_k})\nabla k\right]+G_k-\varepsilon \qquad (7)$$

$$\frac{\partial \varepsilon}{\partial t}+\vec{V}.\nabla\varepsilon=\nabla.\left[(\nu+\frac{\nu_t}{\sigma_\varepsilon})\nabla\varepsilon\right]+C_{1\varepsilon}\frac{\varepsilon}{k}G_k-C_{2\varepsilon}\frac{\varepsilon^2}{k} \qquad (8)$$

$$\mu_t = \rho C_\mu \frac{k^2}{\varepsilon} \qquad (9)$$

Typical constant values were used for the model (k-ε), where C_μ = 0.09, $C_{1\varepsilon}$=1.44, $C_{2\varepsilon}$=1.92, and the diffusion coefficients were σ_ε=1.0, σ_k =1.3

This study relied on a set of dimensionless relationships, equations, and basic criteria to describe the phenomenon of mixed convection heat transfer within the studied cavity. The Reynolds number (Re) represents the effect of forced flow forces, while the Grashof number (Gr) expresses the effect of buoyancy forces resulting from temperature differences. The Richardson number (Ri) is used to compare the effects of natural and forced convection. The Prandtl number (Pr) links the physical properties of the fluid through viscosity and thermal diffusivity. The heat transfer quantity (Q) and the average heat transfer coefficient (h_{ave}) were calculated, followed by the Nusselt number (Nu), which is a key indicator of heat transfer efficiency. In addition, the efficiency coefficient (ε) was used to comprehensively evaluate the performance of the thermal cavity by comparing the actual heat difference with the maximum possible heat difference[32], [33], [34], [35].

$$\mathrm{Re} = \frac{\rho u_{in} L_{ca}}{\mu} \qquad (10)$$

$$Gr = \frac{g\beta(T_h - T_c)L^3_{ca}}{\nu^2} \qquad (11)$$

$$Ri = \frac{Gr}{\mathrm{Re}^2} \qquad (12)$$

$$\mathrm{Pr} = \frac{\nu}{\alpha} = \frac{\rho C_p}{\lambda} \qquad (13)$$

$$Q = \int q'' dA \qquad (14)$$

$$h_{ave} = \frac{Q}{A(T_w - T_f)} \qquad (15)$$

$$Nu_{ave} = \frac{h_{ave} L_{ca}}{\lambda} \qquad (16)$$

$$\varepsilon = \frac{T_o - T_{in}}{T_h - T_{in}} \qquad (17)$$

2.2.2 Procedure of Numerical Solution

Numerical simulations were performed using ANSYS Fluent software to find the temperature and fluid velocity distribution inside the rectangular cavity at different aspect ratios (AR = 0.5, 1, 1.5, and 2) and Reynolds number ranges from Re = 4000 to Re = 22000 with 200 increments between each case.

2.2.3 Mesh Generation

The geometric model was created using ANSYS Design Modeller, with dimensions of L = 2m and height varying according to the AR ratio. A regular Triangular Structured Mesh was generated to ensure accuracy and reduce the number of elements. A grid independence test was conducted, testing three mesh density levels and selecting the mesh that achieves a balance between accuracy and computational time. Figure (3) shows the numerical mesh generation process for a two-dimensional cavity at different aspect ratios (AR=0.5, 1, 1.5, and 2). The mesh resolution and distribution are essential factors in ensuring the accuracy of numerical results when simulating heat transfer by natural convection, as the mesh affects the representation of the flow and temperature distribution within the cavity. An appropriate mesh size was chosen to achieve a balance between numerical accuracy and minimizing computational cost.

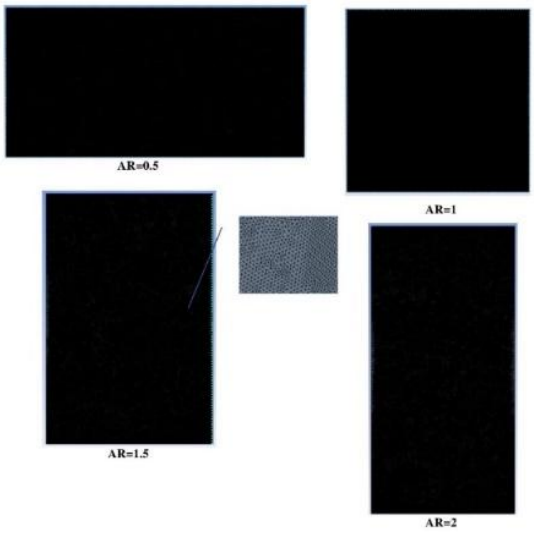

Figure 3. Generating the numerical mesh of the cavity at different aspect ratios.

2.2.4 Validation of Numerical Simulation

The results of the current study were compared with those of Rahman et al. [36], who investigated the effect of Reynolds and Prandtl numbers on mixed convection heat transfer in a square cavity containing a heat-conducting square cylinder at different locations. The comparison showed a high convergence between the Nusselt number results, with the relative error between the two studies ranging from 0.60% to 3.97%. This validation strengthens the validity of the adopted mathematical and physical hypotheses and provides confidence in the analysis of mixed convection heat transfer in rectangular cavities, as shown in Figure (4).

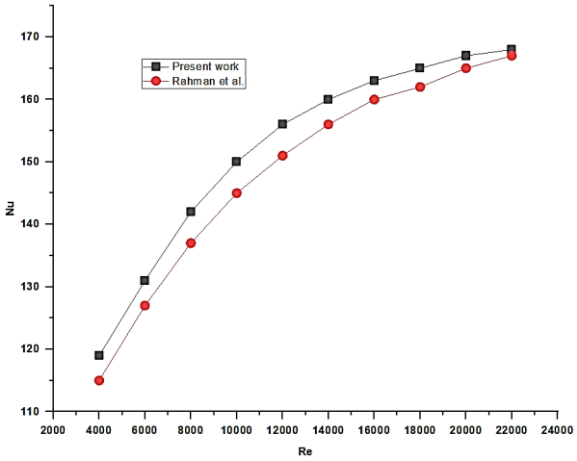

Figure 4. Comparison of the Nusselt number and Reynolds number relationship for the current work versus a previous study.

3. Result and Discussion

3.1 Effect of (Re, Ri, and AR) on Heat Transfer

The numerical results in the three Figures (5-7) clearly demonstrate the behavior of mixed convection heat transfer. Figure (5) shows the relationship between the average Nusselt number (Nu) and the Reynolds number (Re) at different aspect ratios (AR). It is observed that increasing Re from 500 to 2000 leads to a significant increase in Nu. For example, at AR = 1, Nu increased from about 8 to nearly 21 (an increase of approximately 162%), while at AR = 0.5, the increase was smaller, from about 6 to 14 (approximately 133%). This is due to the thinning of the thermal boundary layer and the increased

intensity of the vortices with increasing Re, which improves thermal mixing. Figure (6) shows the variation of Nu with the Richardson number (Ri) at different AR ratios. It is observed that increasing Ri from 0.01 (forced convection dominance) to 10 (natural convection dominance) significantly reduces Nu due to the weakening of the shear forces and the increased thickness of the thermal boundary layer. For example, at AR = 1, Nu decreases from about 20 at Ri = 0.01 to about 9 at Ri = 10 (a decrease of approximately 55%). Figure (7) highlights the same effect of AR at different Reynolds numbers, demonstrating optimal cavity ratios that achieve the highest heat transfer efficiency. For example, at Re = 1000, Nu reaches its highest value at AR = 1, at about 15, while it decreases to about 12 at AR = 2 (a decrease of approximately 20%). At Re = 2000, cavities with lower ARs outperform, with Nu reaching about 22 at AR = 0.5 versus about 20 at AR = 1. In general, these changes are explained physically by the balance of buoyancy and shear forces. At low Re, natural convection effects dominate, resulting in weak mixing, while as Re increases, forced convection increases and enhances internal vortices, increasing heat transfer efficiency. AR also affects the length of the flow path and the distribution of vortices, which determines the intensity of convective mixing and the increase or decrease in Nu values.

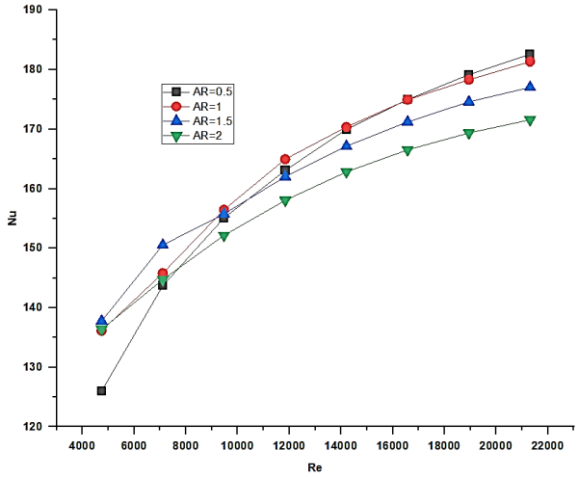

Figure 5. Variation of the average Nusselt number with the Reynolds number at different aspect ratios of a rectangular cavity.

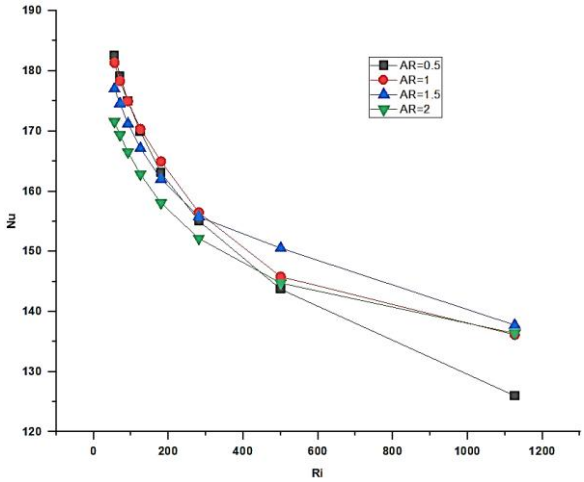

Figure 6. Effect of Richardson number on average Nusselt number at different aspect ratios.

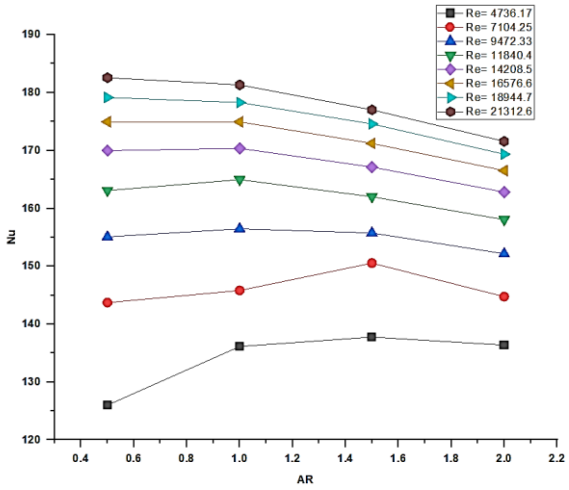

Figure 7. Average Nusselt number changes with aspect ratio for different Reynolds numbers.

3.2 Local Pressure within the Cavity

Figure (8) shows the distribution of local pressure (P) along the hot wall at different heights (H = 0.5, 1, 1.5, and 2 m) for different aspect ratios (AR = 0.5, 1, 1.5, and 2). It is noticeable from the figure that the pressure increases gradually and almost linearly with height, regardless of the AR value, reflecting the effect of gravity on the hydrostatic pressure distribution within the space. The differences between the pressure values at the same height between the different AR cases appear to be very slight, not exceeding about ±0.03 Pa at most points, indicating that the effect of the aspect ratio on the local pressure on the hot wall is secondary. This can be explained physically by the fact that natural convection and mixing within the space lead to slight changes in the density and velocity distributions. However, since the hot wall is thermally constant along its length in all cases, the differences in the pressure distribution are primarily related to a slight difference in the flow pattern near the wall. It can be concluded from the figure that the pressure distribution is mainly governed by the properties of natural convection and the laminar nature of the flow near the wall, and that AR does not cause significant changes in these properties within the study area.

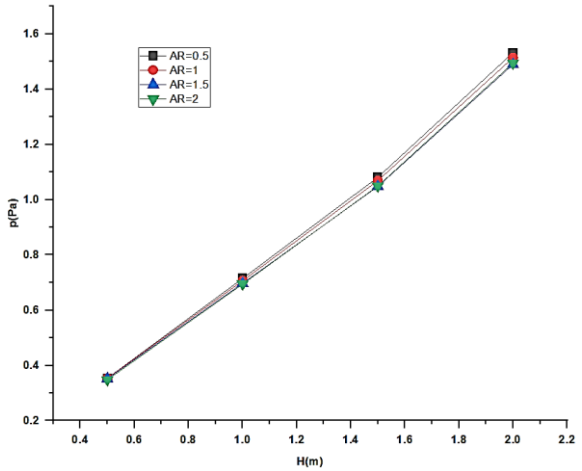

Figure 8. Variation of local pressure with height of a hot wall at different aspect ratios.

3.3 Cooling Effectiveness

The results also showed that the heat transfer efficiency inside the two-dimensional rectangular cavity is clearly affected by the Reynolds number (Re), the Richardson number (Ri), and the aspect ratio (AR). Analyzing the relationship between the efficiency and Re (Figure 9), it was observed that the efficiency

decreases with increasing Re for all values of AR. The efficiency for AR = 1 decreased from 0.281 at Re ≈ 4736 to 0.133 at Re ≈ 21313, a decrease of approximately 52.7%, while the efficiency for AR = 2 decreased from 0.263 to 0.160 for the same range, a decrease of approximately 39.2%. This decrease is attributed to the dominance of the forced convection effect at high speeds, which reduces the effect of natural convection and thus weakens the mixing of thermal layers. In contrast, Figure (10) shows that the efficiency clearly increases with increasing Ri, reflecting the natural convection enhancement of heat exchange efficiency. The efficiency of AR = 1 increased from 0.132 at Ri ≈ 30 to 0.281 at Ri ≈ 1200, an increase of 113%. The efficiency of AR = 2 increased by 66.5% over the same Ri range, indicating that natural convection significantly contributes to the improvement of heat transfer performance. Regarding the effect of AR, the results in Figure (11) show that there are optimal values for the aspect ratio depending on Re. AR = 1 achieved the highest efficiency (0.281) at Re ≈ 4736, while at high Re, such as 21313, AR = 2 became more efficient (0.160) compared to AR = 0.5 (0.133), a difference of 20.3%. This behavior can be explained by the fact that varying AR leads to a change in the flow pattern and vortex distribution within the cavity, which in turn affects heat transfer efficiency. Therefore, the interaction between the effects of Re, Ri, and AR is complex, requiring careful selection of engineering and operational parameters to achieve optimal thermal performance.

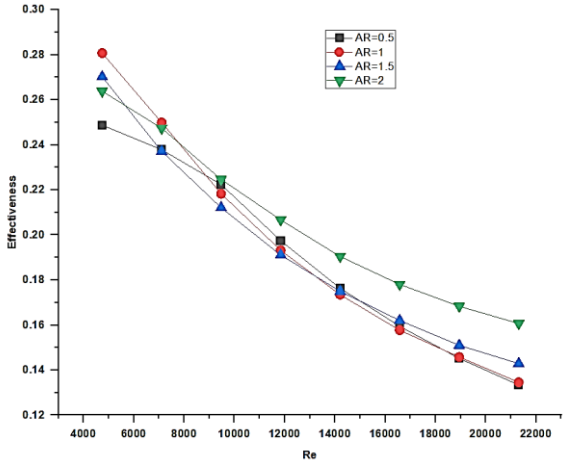

Figure 9. Variation of effectiveness with Reynolds number at different aspect ratios of a rectangular cavity.

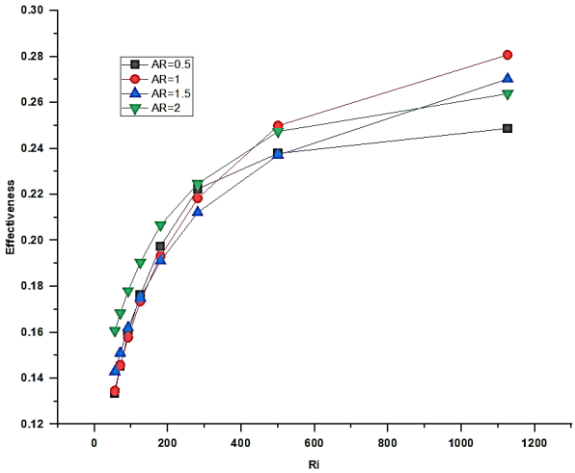

Figure 10. Effect of Richardson number on effectiveness at different aspect ratios.

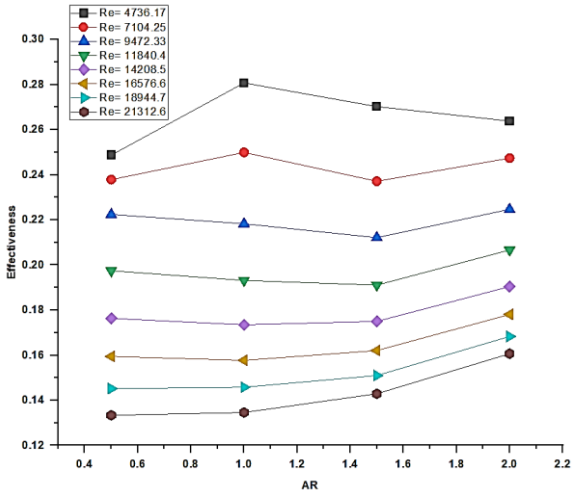

Figure 11. Effectiveness changes with aspect ratio for different Reynolds numbers.

3.4 Qualitative Analysis of Temperature and Velocity Fields

Figures (12) and (13) represent the numerical distribution of both temperatures and velocity vectors inside the rectangular cavity at different aspect ratios (AR = 0.5, 1, 1.5, and 2). Figure (12) shows that the temperature distribution is significantly affected by changes in AR, as the pattern of the thermal gradient and thermal boundary layers changes. At AR = 0.5, a limited thermal gradient appears on the hot wall due to the short height of the cavity. This weakens the development of natural convection currents and causes heat to remain concentrated near the upper surface, explaining the reduced heat exchange efficiency in this case. In contrast, at AR = 2, a strong, vertically extended thermal gradient and a thin thermal layer on the hot wall are evident. This reflects the development of natural convection within the cavity, leading to improved thermal mixing and increased efficiency. Figure (13) shows the velocity vectors inside the cavity, which illustrate the internal flow pattern. At AR = 0.5, a complex flow pattern is formed, including multiple superimposed vortices, indicating relative turbulence in the flow. However, this does not contribute to efficient heat mixing due to the short vertical distance for these vortices to develop. At AR = 1, the vortices begin to become more regular, showing a pronounced rotational motion on the hot wall and an upward flow on the cold surface. As AR increases to 1.5 and 2, a single, large, dominant vortex with a horizontal or oblique axis forms, covering most of the cavity. This indicates a stable mixed convection pattern and improved heat transfer due to stronger rotation and more uniform heat mixing. Thus, it is clear that increasing AR contributes to enhancing both the thermal gradient and eddy current development, which positively impacts the efficiency of heat exchange within the cavity. The relationship between the space shape and flow pattern also demonstrates the importance of geometric design in improving thermal performance.

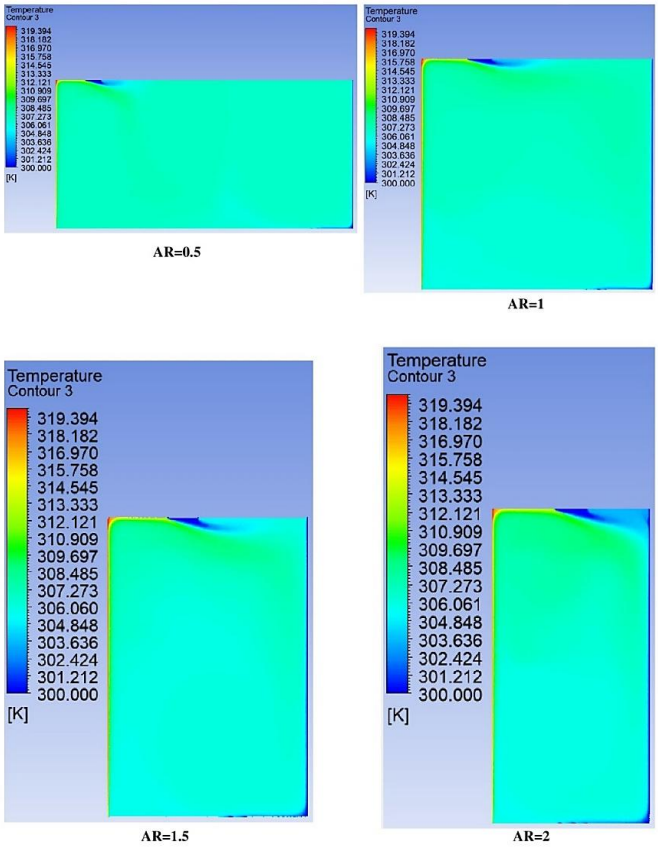

Figure 12. Temperature distribution inside the cavity at different aspect ratios (AR = 0.5, 1, 1.5, 2).

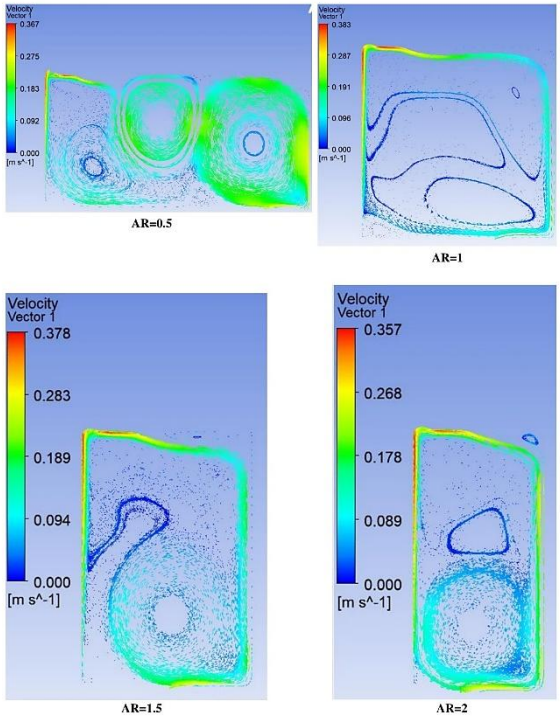

Figure 13. Distribution of velocity vectors inside the cavity at different aspect ratios (AR = 0.5, 1, 1.5, 2).

4. Conclusions

This work investigated mixed convection heat transfer within a rectangular cavity, focusing on the effect of varying the aspect ratio (AR) on the thermal and hydrodynamic performance of the system. The left wall of the cavity was heated, and the right wall was cooled, with an air inlet at the top and an outlet at the bottom, while the remaining walls were thermally insulated. The flow and temperature behavior were analyzed using numerical simulations, varying the Reynolds number (Re) and Richardson number (Ri), to determine the optimal geometric configurations that achieve the highest thermal efficiency. Based on the results extracted from the graphs, flowline analysis, and heat contour, the following conclusions can be drawn: The results showed that the Nusselt number (Nu) increased with increasing Reynolds number for all studied dimensionality ratios, indicating improved heat transfer with enhanced forced convection within the cavity. At high Reynolds number values, the highest Nusselt number values were recorded at an AR = 0.5 dimensionality ratio, while AR = 1 and AR = 1.5 were more efficient at lower Reynolds number values. The results also showed that increasing the Richardson number, which reflects the increased effect of natural convection compared to forced convection, led to a decrease in the Nusselt number, indicating reduced heat transfer efficiency under natural convection. Conversely, the highest Nusselt number values were recorded at lower Richardson number values, confirming the effectiveness of forced convection in improving heat transfer. In terms of overall thermal performance, the best Nusselt number values were observed at dimension ratios AR = 1 and AR = 1.5 in most cases, indicating an optimal operating point for these ratios. Conversely, very low or very high dimension ratio values resulted in reduced heat transfer efficiency. Regarding the pressure distribution within the cavity, the pressure increased with increasing height H, regardless of the dimension ratio, with very slight differences between the various cases, suggesting that the effect of dimension ratio on pressure distribution is limited. The results also showed that efficiency decreases with increasing Reynolds number due to increased flow velocity and decreased air residence time within the cavity. Conversely, efficiency increases with increasing Richardson number, as the natural convection allows for a longer and more uniform thermal contact time. A dimensionality ratio (AR) of 1 was found to achieve the best efficiency in most cases, particularly at high Richardson number values. Heat distribution maps revealed a clear thermal gradient on the heated wall, particularly at large aspect ratios such as 1.5 and 2, enhancing the effect of natural convection. Flow line maps also showed the formation of multiple vortices at aspect ratio AR = 0.5, compared to one or two more regular vortices at aspect ratios AR = 1 and AR = 1.5, contributing to improved heat transfer through a more uniform flow mechanism.
As a future proposal, it is recommended to apply the studied mixed flow model to automotive HVAC systems, taking into account the actual inlet and outlet locations, unstable operating conditions, and the impact of passenger heat loads, with the aim of improving thermal comfort and increasing energy efficiency in vehicles.

Declaration of AI and AI assisted technologies in the writing process
In preparing this study, the authors used ChatGPT, a tool developed by OpenAI, to improve text clarity and readability. After using this tool, the authors carefully reviewed the content and made the necessary edits, and they assume full responsibility for all content presented in this work.

Declaration of Competing Interest
The authors acknowledge that there are no conflicting financial interests or personal relationships that could have influenced the findings or work presented in this study.

Acknowledgement
The authors acknowledge that this article received no financial or moral support from any academic or research institution, and was completed entirely through their own efforts.

References

[1] F. Karimi, H. Xu, Z. Wang, M. Yang, and Y. Zhang, "Numerical simulation of steady mixed convection around two heated circular cylinders in a square enclosure," *Taylor & FrancisF Karimi, H Xu, Z Wang, M Yang, Y ZhangHeat Transfer Engineering, 2016•Taylor & Francis*, vol. 37, no. 1, pp. 64–75, Jan. 2016, doi: https://doi.org/10.1080/01457632.2015.1042343.

[2] F. M. Azizul, A. I. Alsabery, I. Hashim, and A. J. Chamkha, "Heatline visualization of mixed convection inside double lid-driven cavity having heated wavy wall: FM Azizul et al.," *SpringerFM Azizul, AI Alsabery, I Hashim, AJ ChamkhaJournal of Thermal Analysis and Calorimetry, 2021•Springer*, vol. 145, no. 6, pp. 3159–3176, Sep. 2021, doi: https://doi.org/10.1007/S10973-020-09806-5.

[3] S. Kumar, K. M. Gangawane, and H. F. Oztop, "A numerical study of mixed convection in a two-sided lid-driven tall cavity containing a heated triangular block for non-Newtonian power-law fluids," *Wiley Online LibraryS Kumar, KM Gangawane, HF OztopHeat Transfer, 2021•Wiley Online Library*, vol. 50, no. 5, pp. 4806–4829, Jul. 2021, doi: https://doi.org/10.1002/HTJ.22103.

[4] N. Billah, M. Khan, M. Rahman, … M. A.-A. C., and undefined 2017, "Numerical study of mixed convection heat transfer enhancement in a channel with active flow modulation," *pubs.aip.org*, Accessed: Apr. 21, 2026. [Online]. Available: https://pubs.aip.org/aip/acp/article-abstract/1851/1/020104/886002

[5] 0.781Q1SJR Q1; 0.781NAABS NANAABDC NAChinese Journal of Chemical EngineeringKM Gangawane, B. M.-C. J. of Chemical, and undefined 2017, "Mixed convection characteristics in lid-driven cavity containing heated triangular block," *Elsevier*, Accessed: Apr. 21, 2026. [Online]. Available: https://www.sciencedirect.com/science/article/pii/S100495411631206X

[6] J. F. Hinojosa, N. A. Rodríguez, and J. Xamán, "Heat transfer and airflow study of turbulent mixed convection in a ventilated cavity," *journals.sagepub.comJF Hinojosa, NA Rodríguez, J XamánJournal of Building Physics, 2016•journals.sagepub.com*, vol. 40, no. 3, pp. 204–234, Nov. 2016, doi: https://doi.org/10.1177/1744259115611640.

[7] 1.16Q1SJR Q1; 1.16NAABS NANAABDC NAInternational Journal of Thermal SciencesL Koufi, Z. Younsi, Y. Cherif, H. N.-I. J. of Thermal, and undefined 2017, "Numerical investigation of turbulent mixed convection in an open cavity: Effect of inlet and outlet openings," *ElsevierL Koufi, Z Younsi, Y Cherif, H NajiInternational Journal of Thermal Sciences, 2017•Elsevier*, Accessed: Apr. 21, 2026. [Online]. Available: https://www.sciencedirect.com/science/article/pii/S1290072916312467

[8] 0.432Q2SJR Q2; 0.432NAABS NANAABDC NAFluidsA Carozza - Fluids and undefined 2018, "Numerical study on mixed convection in ventilated cavities with different aspect ratios," *mdpi.comA CarozzaFluids, 2018•mdpi.com*, Accessed: Apr. 21, 2026. [Online]. Available: https://www.mdpi.com/2311-5521/3/1/11

[9] 0.444Q2SJR Q2; 0.444NAABS NANAABDC NAHeat Transfer EngineeringBP Geridonmez, H. O.-H. T. Engineering, and undefined 2021, "Mixed convection heat transfer in a lid-driven cavity under the effect of a partial magnetic field," *Taylor & FrancisBP Geridonmez, HF OztopHeat Transfer Engineering, 2021•Taylor & Francis*, pp. 1–13, 2020, doi: https://doi.org/10.1080/01457632.2020.1792622.

[10] N. S. Gibanov, M. A. Sheremet, M. A. Ismael, and A. J. Chamkha, "Mixed convection in a ventilated cavity filled with a triangular porous layer," *SpringerNS Gibanov, MA Sheremet, MA Ismael, AJ ChamkhaTransport in Porous Media, 2017•Springer*, vol. 120, no. 1, pp. 1–21, Oct. 2017, doi: https://doi.org/10.1007/S11242-017-0888-Y.

[11] H. Doghmi, B. Abourida, L. Belarche, M. Sannad, and M. Ouzaouit, "Effect of the inlet opening on mixed convection inside a 3-D ventilated cavity," *doiserbia.nb.rsH Doghmi, B Abourida, L Belarche, M Sannad, M OuzaouitThermal science, 2018•doiserbia.nb.rs*, vol. 22, no. 6A, pp. 2413–2424, doi: https://doi.org/10.2298/TSCI170126121D.

[12] 1.299Q1SJR Q1; 1.299NAABS NANAABDC NAInternational Journal of Heat and Mass TransferR Zhu, P. Zhou, J. Li, C. Z.-I. J. of H. and Mass, and undefined 2020, "CFD model evaluation in mixed convection with high Richardson number," *ElsevierR Zhu, P Zhou, J Li, CQ ZhouInternational Journal of Heat and Mass Transfer, 2020•Elsevier*, Accessed: Apr. 21, 2026. [Online]. Available: https://www.sciencedirect.com/science/article/pii/S0017931019346629

[13] 1.579Q1SJR Q1; 1.579NAABS NANAABDC NAApplied Thermal EngineeringKL Lee, A. Chinnici, M. Jafarian, … M. A.-A. T., and undefined 2019, "The influence of wall temperature distribution on the mixed convective losses from a heated cavity," *ElsevierKL Lee, A Chinnici, M Jafarian, M Arjomandi, B Dally, G NathanApplied Thermal Engineering, 2019•Elsevier*, Accessed: Apr. 21, 2026. [Online]. Available: https://www.sciencedirect.com/science/article/pii/S1359431118360435

[14] N. A. Bakar, A. Karimipour, and R. Roslan, "Effect of magnetic field on mixed convection heat transfer in a lid-driven square cavity," *Wiley Online LibraryNA Bakar, A Karimipour, R RoslanJournal of Thermodynamics, 2016•Wiley Online Library*, vol. 2016, 2016, doi: https://doi.org/10.1155/2016/3487182.

[15] 1.076Q1SJR Q1; 1.076NAABS NANAABDC NAAin Shams Engineering JournalSD Farahani, A. Alizadeh, M. Tashkandi, … L. K.-A. S. E., and undefined 2024, "Artificial intelligence approach in mixed convection heat transfer under transverse mechanical vibrations in a rectangular cavity," *ElsevierSD Farahani, A Alizadeh, MA Tashkandi, L Kolsi, A KarimipourAin Shams Engineering Journal, 2024•Elsevier*, Accessed: Apr. 21, 2026. [Online]. Available: https://www.sciencedirect.com/science/article/pii/S2090447924003873

[16] 0.498Q2SJR Q2; 0.498NAABS NANAABDC NAMathematicsF Mebarek-Oudina, H. Laouira, A. Hussein, M. O.- Mathematics, and undefined 2022, "Mixed convection inside a duct with an open trapezoidal cavity equipped with two discrete heat sources and moving walls," *mdpi.comF Mebarek-Oudina, H Laouira, AK Hussein, M Omri, A Abderrahmane, L Kolsi, U BiswalMathematics, 2022•mdpi.com*, Accessed: Apr. 21, 2026. [Online]. Available: https://www.mdpi.com/2227-7390/10/6/929

[17] N. Ismael, … A. H.-J. of H., and undefined 2020, "Effect of driven sidewalls on mixed convection in an open trapezoidal cavity with a channel," *asmedigitalcollection.asme.orgMA Ismael, AK Hussein, F Mebarek-Oudina, L KolsiJournal of Heat Transfer, 2020•asmedigitalcollection.asme.org*, Accessed: Apr. 21, 2026. [Online]. Available: https://asmedigitalcollection.asme.org/heattransfer/article-abstract/142/8/082601/1083314

[18] 1.028Q1SJR Q1; 1.028NAABS NANAABDC NAThermal Science and Engineering ProgressSK Mandal, A. Deb, D. S.-T. S. and E. Progress, and undefined 2019, "Mixed convective heat transfer with surface radiation in a rectangular channel with heat sources in presence of heat spreader," *Elsevier*, Accessed: Apr. 21, 2026. [Online]. Available: https://www.sciencedirect.com/science/article/pii/S2451904919301106

[19] F. Mebarek-Oudina, H. Laouira, A. Aissa, A. K. Hussein, and M. El Ganaoui, "Convection heat transfer analysis in a channel with an open trapezoidal cavity: Heat source locations effect," *matec-conferences.orgF Mebarek-Oudina, H Laouira, A Aissa, AK Hussein, M El GanaouiMATEC Web of Conferences, 2020•matec-conferences.org*, doi: https://doi.org/10.1051/matecconf/202033001006.

[20] 0.393Q2SJR Q2; 0.393NAABS NANAABDC NAEngineering ComputationsMA Ismael - Engineering Computations and undefined 2017, "Numerical solution of mixed convection in a lid-driven cavity with arc-shaped moving wall," *emerald.comMA IsmaelEngineering Computations, 2017•emerald.com*, Accessed: Apr. 21, 2026. [Online]. Available: https://www.emerald.com/ec/article-abstract/34/3/869/256489

[21] 1.171Q1SJR Q1; 1.171NAABS NANAABDC NAResults in EngineeringMN Islam, U. Aziz, R. Karmaker, S. A.-R. in Engineering, and undefined 2025, "Numerical investigation of mixed convection heat transfer enhancement in a square cavity with a hump-shaped heated bottom wall," *ElsevierMN Islam, UI Aziz, R Karmaker, SF AhmedResults in Engineering, 2025•Elsevier*,

Accessed: Apr. 21, 2026. [Online]. Available: https://www.sciencedirect.com/science/article/pii/S2590123025034656

[22] 0.68Q1SJR Q1; 0.68NAABS NANAABDC NAJournal of EngineeringSA Ali, S. R.-J. of Engineering, and undefined 2024, "Experimental investigation of forced convection in plain or partly inserted square channel with porous media," *joe.uobaghdad.edu.iqSA Ali, SA RasheedJournal of Engineering, 2024•joe.uobaghdad.edu.iq*, vol. 2024, no. 4, p. 30, doi: https://doi.org/10.31026/j.eng.2024.04.07.

[23] N. Al-Akam, H. Kadhim, S. A.-… F. D. Letters, and undefined 2025, "Numerical Analysis for the Airflow Behaviour around Vortex Generators Used for Air-Cooling Technologies Considering Rotation," *researchgate.netA Al-Akam, HK Kadhim, SA Ali, AM Al JubooriComputational Fluid Dynamics Letters, 2025•researchgate.net*, vol. 17, pp. 127–144, 2025, doi: https://doi.org/10.37934/cfdl.17.9.127144.

[24] 0.937Q1SJR Q1; 0.937NAABS NANAABDC NAInternational Journal of RefrigerationS Duret, D. Flick, J. M.-I. J. of Refrigeration, and undefined 2025, "Characterising airflow and heat transfer within a multi-package of horticultural produce using a validated CFD model," *ElsevierS Duret, D Flick, J MourehInternational Journal of Refrigeration, 2025•Elsevier*, Accessed: Apr. 21, 2026. [Online]. Available: https://www.sciencedirect.com/science/article/pii/S014070072400433X

[25] 1.429Q1SJR Q1; 1.429NAABS NANAABDC NAInternational journal of thermofluidsMD Afifi, A. Jahangiri, M. A.-I. journal of thermofluids, and undefined 2025, "Investigation of natural convection heat transfer in MHD fluid within a hexagonal cavity with circular obstacles," *ElsevierMD Afifi, A Jahangiri, M AmeriInternational journal of thermofluids, 2025•Elsevier*, Accessed: Apr. 21, 2026. [Online]. Available: https://www.sciencedirect.com/science/article/pii/S2666202724004634

[26] A. R. Al-Badri, A. A. Y. Al-Waaly, G. Saha, T. Saha, and S. C. Saha, "Improving Thermal Performance in Building Heating, Ventilation, and Air Conditioning Systems: A Study of Natural Convection and Entropy in Plus-Shaped Cavity," *Wiley Online LibraryAR Al-Badri, AAY Al-Waaly, G Saha, T Saha, SC SahaHeat Transfer, 2025•Wiley Online Library*, vol. 54, no. 3, pp. 2235–2250, May 2025, doi: https://doi.org/10.1002/HTJ.23288.

[27] 1.579Q1SJR Q1; 1.579NAABS NANAABDC NAApplied Thermal EngineeringZ Gong, J. Ren, P. Si, L. Shi, Z. W.-A. T. Engineering, and undefined 2025, "Effects of fluid–structure interaction on natural convection heat transfer in a square cavity divided by vertically flexible walls," *ElsevierZ Gong, J Ren, P Si, L Shi, Z WangApplied Thermal Engineering, 2025•Elsevier*, Accessed: Apr. 21, 2026. [Online]. Available: https://www.sciencedirect.com/science/article/pii/S1359431125002078

[28] 0.451Q2SJR Q2; 0.451NAABS NANAABDC NANumerical Heat Transfer, P. A. A. Miranda, D. S.-T.-… H. Transfer, P. A, and undefined 2025, "Turbulence models performance to predict fluid mechanics and heat transfer characteristics of fluids flow in micro-scale channels," *Taylor & FrancisEP Miranda, DF Sempértegui-Tapia, CA ChávezNumerical Heat Transfer, Part A: Applications, 2025•Taylor & Francis*, vol. 86, no. 13, pp. 4353–4373, 2025, doi: https://doi.org/10.1080/10407782.2024.2318001.

[29] 0.874Q1SJR Q1; 0.874NAABS NANAABDC NAScientific ReportsV Chandrakar, A. Bhattad, P. Samal, J. S.-S. Reports, and undefined 2025, "A study on different methods to change the Rayleigh number in the analysis of heat transfer," *nature.comV Chandrakar, A Bhattad, P Samal, JR Senapati, AK KashyapScientific Reports, 2025•nature.com*, doi: https://doi.org/10.1038/s41598-025-11120-9.

[30] 0.736Q1SJR Q1; 0.736NAABS NANAABDC NAInternational Journal of Environmental Science and TechnologyA Abdi, O. Abessi, E. K.-I. J. of Environmental, and undefined 2023, "The effect of opening on the enhancement of natural ventilation in indoor spaces," *SpringerA Abdi, O Abessi, E KhavasiInternational Journal of Environmental Science and Technology*,

2023•Springer, vol. 20, no. 2, pp. 1875–1886, Feb. 2023, doi: https://doi.org/10.1007/S13762-022-04720-9.

[31] N. Duong, T. Hoang, … H. T.-V. C. on, and undefined 2023, "Simumaltion of Natural Convection Flow for Vertical Heated Rod Using ANSYS/Fluent," *inis.iaea.orgTT Duong, TH Hoang, HT Truong, CT TranVietnam Conference on Nuclear Science and Technology VINANST-15. Agenda, 2023•inis.iaea.org*, Accessed: Apr. 21, 2026. [Online]. Available: https://inis.iaea.org/records/1hkrd-btr11

[32] S. O. Giwa, M. Sharifpur, M. H. Ahmadi, and J. P. Meyer, "A review of magnetic field influence on natural convection heat transfer performance of nanofluids in square cavities: SO Giwa et al.," *SpringerSO Giwa, M Sharifpur, MH Ahmadi, JP MeyerJournal of Thermal Analysis and Calorimetry, 2021•Springer*, vol. 145, no. 5, pp. 2581–2623, Sep. 2021, doi: https://doi.org/10.1007/S10973-020-09832-3.

[33] J. Zheng, L. Zhang, H. Yu, Y. Wang, and T. Zhao, "Study on natural convection heat transfer in a closed cavity with hot and cold tubes," *journals.sagepub.comJ Zheng, L Zhang, H Yu, Y Wang, T ZhaoScience Progress, 2021•journals.sagepub.com*, vol. 104, no. 2, 2021, doi: https://doi.org/10.1177/00368504211020965.

[34] 0.944Q1SJR Q1; 0.944NAABS NANAABDC NAColloids and Surfaces A: Physicochemical and Engineering AspectsZ Tian, Z. Tang, C. Qi, L. Chen, Y. W.-C. and S. A, and undefined 2022, "Natural convection heat transfer characteristics of sinusoidal cavities filled with nanofluids," *ElsevierZ Tian, Z Tang, C Qi, L Chen, Y WangColloids and Surfaces A: Physicochemical and Engineering Aspects, 2022•Elsevier*, Accessed: Apr. 21, 2026. [Online]. Available: https://www.sciencedirect.com/science/article/pii/S0927775722010640

[35] 1.061Q1SJR Q1; 1.061NAABS NANAABDC NACase Studies in Thermal EngineeringY Cao, H. Almasi, C. Soto, O. Akbari, … G. A.-C. S. in T., and undefined 2025, "Mixed convection of nanofluid flow in a circular lid-driven cavity affected by attack angle changes: A numerical simulation," *ElsevierY Cao, H Almasi, C Soto, OA Akbari, G Ahmadi, S Esmaeili, Y KhairyCase Studies in Thermal Engineering, 2025•Elsevier*, Accessed: Apr. 21, 2026. [Online]. Available: https://www.sciencedirect.com/science/article/pii/S2214157X25013711

[36] 0.197Q4SJR Q4; 0.197NAABS NANAABDC NAJournal of Mechanical EngineeringS Saha - Journal of Mechanical Engineering and undefined 2009, "A numerical study of mixed convection in a square cavity with a heat conducting square cylinder at different locations," *academia.eduS SahaJournal of Mechanical Engineering, 2009•academia.edu*, Accessed: Apr. 21, 2026. [Online]. Available: https://www.academia.edu/download/49486586/A_Numerical_Study_of_Mixed_Convection_in20161009-28472-1qjhe80.pdf

APPENDIX

List of Nomenclature

Symbol	Definition
AR	Aspect Ratio
Cp	Heat capacity, (J/kg. K)
FVM	Finite Volume Method
g	Gravity acceleration (m/s^2)
Gr	Grashof number
H	Vehicle cabin height, (m)
h	Heat transfer coefficient, (W/m^2. K)
HVAC	Heating Ventilation Air Conditioning
L	Vehicle cabin length, (m)
Nu	Nusselt number

p	Airflow pressure (Pa)
Pr	Prandtl number
Q	Heat transfer rate (W)
Ra	Rayleigh number
Re	Reynolds number
Ri	Richardson number
T	Airflow Temperature, (K)
U	Airflow velocity, (m/s)
u and v	Component velocity in x and y direction, respectively, (m/s)
x and y	Horizontal and vertical coordinate in a two-dimensional cavity, respectively
μ	Airflow dynamics viscosity, (Pa.s)
β	Airflow thermal expansion coefficient, (1/K)
ε	Effectiveness
λ	Airflow thermal conductivity, (W/m.K)
ρ	Airflow density, (kg/m^3)
υ	Airflow kinematic viscosity, (m^2/s)

List of Subscripts

ave	Average
c	Cold
ca	Characteristic
f	fluid
h	Hot
i	Inlet
o	outlet
w	Wall